JCTC Journal of Chemical Theory and Computation

Revisiting Hydrogen [1,5] Shifts in Cyclopentadiene and Cycloheptatriene as Bimolecular Reactions

Shinichi Yamabe,* Noriko Tsuchida, and Shoko Yamazaki

Department of Chemistry, Nara University of Education, Takabatake-cho, Nara 630-8528, Japan

Received March 11, 2005

Abstract: Hydrogen [1,5] shifts are pericyclic reactions and take place typically in 1,3-pentadiene. However, because of structure restriction, the symmetry-allowed thermal reactions of 1,3-cyclopentadiene (CPD) and 1,3,5-cycloheptatriene (CHT) suffer large energy barriers, $\Delta U^{\ddagger} = +26.9$ kcal/mol and $\Delta U^{\ddagger} = +37.5$ kcal/mol by density-functional theory (B3LYP/6-31G*) calculations, respectively. This theoretical study has shown that exo [4+2] and [6+4] cycloadduct dimers involve novel hydrogen-shift channels. After hydrogen migration, one-center adducts are obtained, which undergo Cope rearrangements leading to the second one-center adducts. From the intermediates, reverse routes lead to CPD and CHT with [1,5] migrated hydrogens. A correlation between cycloadditions and [1,5] and [3,3] sigmatropic rearrangements in pericyclic reactions is also discussed.

Introduction

Pericyclic reactions were defined by Woodward and Hoffmann as reactions in which all first-order changes in bonding relationships take place concertedly.[1] Representative pericyclic reactions are cycloadditions, [1,5] and [3,3] sigmatropic shifts, cheletropic additions and eliminations, and electrocyclizations. These reactions involve π-electron conjugated systems consisting of mainly carbon and hydrogen atoms, and they are fundamental in organic reactions. The pathways of pericyclic reactions have been explained in terms of the frontier orbital theory.[2]

The Diels−Alder (DA) reaction ([4+2] cycloaddtion) and hydrogen [1,5] shift are "symmetry allowed", and for these reactions, many ab initio calculations have been reported.[3] For the (butadiene−ethylene) DA reaction, predicted transition-state (TS) geometry with the *Cs* symmetry was obtained. A [1,5] sigmatropic shift of 1,3-pentadiene was calculated, and the concerted and suprafacial hydrogen shift was confirmed.[4] Furthermore, extensive studies and calculations of the pericyclic reactions have been performed.[5] Most calculation results for those reactions support the Woodward−Hoffmann rule and the frontier molecular orbital (FMO) theory.

Scheme 1. Dual Reactivity of 1,3-Cyclopentadiene (CPD). *T* Stands for the Temperature

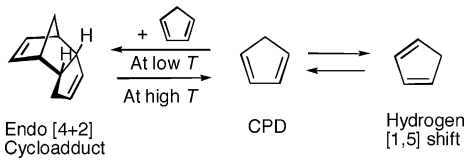

1,3-Cyclopentadiene (CPD) was first used for [4+2] cycloadditions by Diels and Alder.[6] Since then, CPD is the representative diene for DA reactions. Dimerization of CPD gives an endo cycloadduct, dicyclopentadiene.[7] At the same time, CPD undergoes a hydrogen [1,5] sigmatropic shift readily at room temperature (Scheme 1).[8]

Various TS structures for the hydrogen [1,5] shift in CPD have been reported.[9] So far, the two reactions in Scheme 1 have been treated separately.[3,7,10] The hydrogen [1,5] shift in a linear diene 1,3-pentadiene may occur readily[5] owing to the flexible structure of terminal methyl and methylene groups. On the other hand, the methylene C−H bond of CPD cannot be directed to the 4-position methine carbon in the C−H····C alignment owing to ring strain. That is, cleavage of the C−H bond may not accompany the bond interchange in the σ direction.

It appears curious that the hydrogen [1,5] shift of the ring strained structure in CPD has an activation energy (E_a =

* Corresponding author e-mail: yamabes@nara-edu.ac.jp.

10.1021/ct0500646 CCC: $30.25
Published on Web 08/06/2005

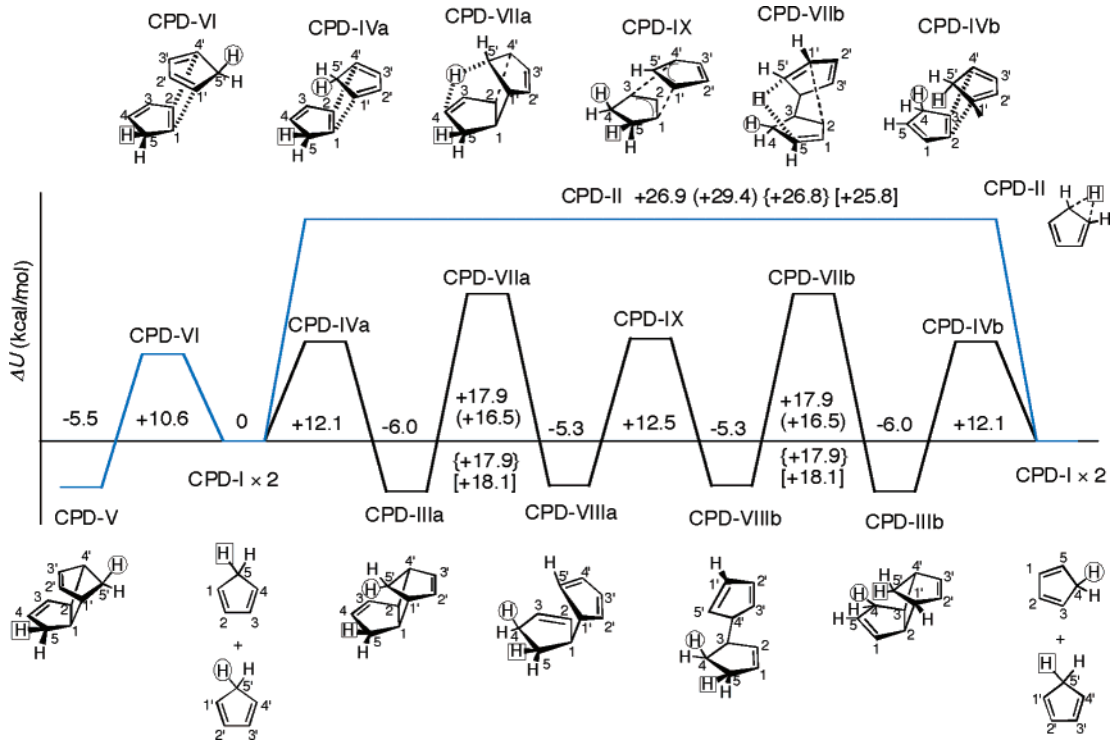

Figure 1. Changes of sums of electronic and zero-point energies (RB3LYP/6-31G*) of [4+2] cycloadditions and Cope and hydrogen [1,5] sigmatropic shifts of CPDs. Energies in parentheses were calculated by QCISD(T)/6-311G(d,p)//RB3LYP/6-31G* [QCISD(T) electronic energies and RB3LYP zero-point vibrational energies]. Those in braces { } were calculated by RB3LYP/6-31G* with the Onsager's reaction field, and those in brackets [ ] were calculated by RB3LYP/6-31G* with polarization functions on the migrating hydrogen atoms.

24.3 kcal/mol)[11] of ca. 10 kcal/mol smaller than that (E_a = 35.4 kcal/mol)[12] of the flexible structure in 1,3-pentadiene. Curiosity lies also in the computational data of activation energies. Jensen and Houk reported 34 kcal/mol[5g] for the hydrogen shift of 1,3-pentadiene, which is in good agreement with experimental data, 35.4 kcal/mol.[12] On the other hand, Okajima and Imafuku reported 28 kcal/mol for the hydrogen shift of CPD,[9d] while the experimental data gives 24.3 kcal/mol.[11] The overestimate of the calculated energy is not explicable, because RB3LYP tends to underestimate the activation energy of some proton- and hydrogen-shift reactions.[13] In this study, bimolecular processes to ensure the bond exchange have been examined for CPD, CHT, and their methyl-substituted reactants, Me-CPD and Me-CHT.

Computational Methods

The density-functional theory (DFT) calculations using the B3LYP hybrid functional[14] and the 6-31G* basis sets (RB3LYP/6-31G*) were carried out by the Gaussian 98 program package[15] in order to investigate the reaction paths of cycloadditions and rearrangements of CPD, CHT, Me-CPD, and Me-CHT. The sums of electronic and zero-point energies of all the species were obtained by vibrational analyses, and they were used as internal energies, U (T = 0 K). To check the above-mentioned underestimation of the activation energy by RB3LYP/6-31G*, QCISD(T)/6-311G-(d,p) single-point calculations were also carried out for key TS geometries.

The CPD and Me-CPD reactions are usually carried out in CCl_4 solvent, while those of CHT and Me-CHT are done in the gas phase (by the temperature over their boiling point). For the CPD and Me-CPD ones, the solvent effect was taken into account for the key species by the Onsager's reaction field approximation[16] with the dielectric constant = 2.228 (CCl_4). The solvent-effect-containing data are shown in braces { }, see Figure 1.

The p-type polarization function on the migrating hydrogen might play an important role in the calculated energies. To check the role, the function was added to the 31G (in 6-31G*) of only the migrating hydrogen. The key species were recalculated by the augmented basis set. The data of this augmented basis set are shown in square brackets [ ], see Figure 1.

Results and Discussion

A Bimolecular Process for the Hydrogen [1,5] Shift in CPD. We have considered that a bimolecular multistep reaction containing cycloaddition and hydrogen shifts can involve a suitable conformation for the bond interchange using a molecular model. These results of the energy changes are shown in Figure 1. The optimized geometries of TS structures CPD-II, CPD-IVa, CPD-VIIa, and CPD-IX are shown in Figures 2−5, respectively. The optimized energy minimum and TS geometries of CPD-I (Figure S1), CPD-IIIa,b (Figures S2 and S8), CPD-IVb (Figure S9), CPD-V (Figure S4), CPD-VI (Figure S3), CPD-VIIb (Figure S7) and CPD-VIIIa,b (Figures S5 and S6) are shown in the Supporting Information. Activation energies $\Delta U^{\ddagger}$ are calculated from the relative internal energies ΔU. As expected, the kinetically most favorable reaction is the endo [4+2] cycloaddition

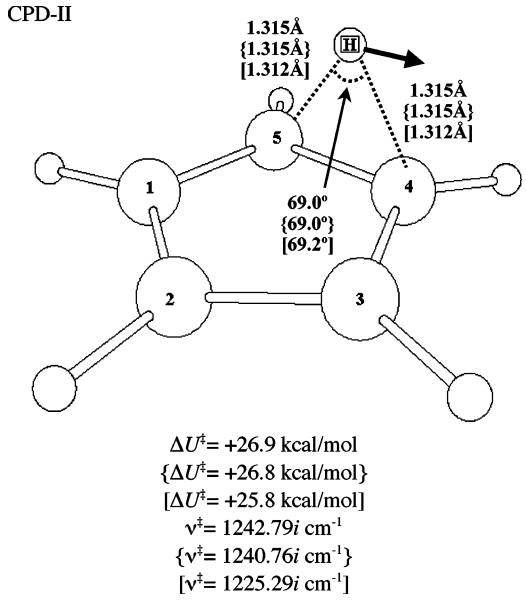

Figure 2. TS of the direct hydrogen [1,5] shift, CPD-II. $\nu^{\ddagger}$ stands for a frequency in vibrational analysis.

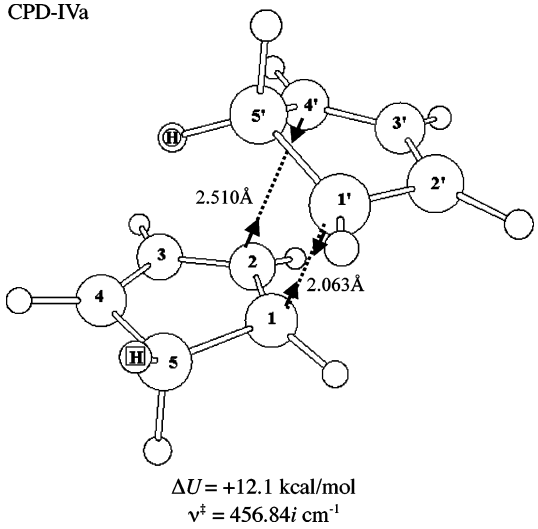

Figure 3. TS of the exo [4+2] cycloaddition, CPD-IVa. The circle and boxed hydrogens are also shown in Figure 1.

Scheme 2. Two CPD Molecules before and after the New Bimolecular Process in Figure 1

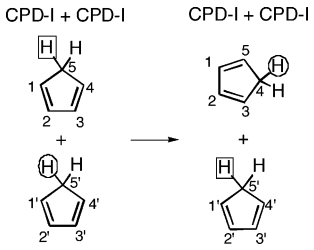

(CPD-VI; $\Delta U^{\ddagger} = +10.6$ kcal/mol) of two CPDs. However, the cycloadduct (CPD-V) is less stable than two reactants (CPD-I × 2, CPDs) in Gibbs free energy difference (Figure 6; $\Delta G = +1.4$ kcal/mol). The direct hydrogen shift (CPD-II; $\Delta U^{\ddagger} = +26.9$ kcal/mol) is the most unfavorable, and the $\Delta U^{\ddagger}$ is larger than the experimentally obtained activation energy ($E_a = 24.3$ kcal/mol).[11] The QCISD(T)/6-311G(d,p) $\Delta U^{\ddagger} = 29.4$ kcal/mol is larger than E_a. A route to the exo

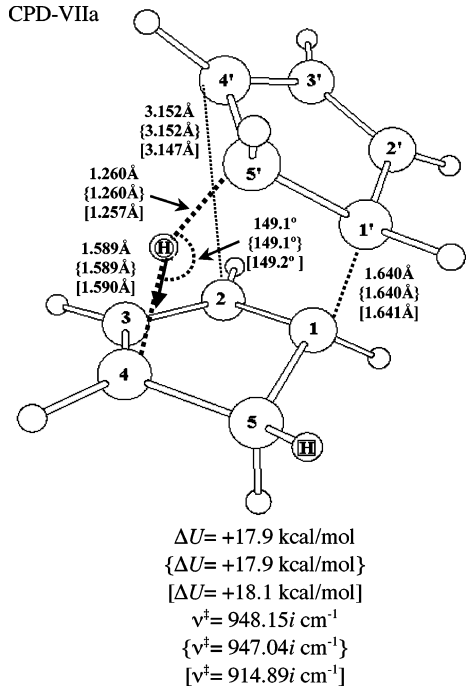

Figure 4. TS of the hydrogen shift from the exo [4+2] adduct (CPD-IIIa) to the one-center adduct intermediate (CPD-VIIIa), CPD-VIIa.

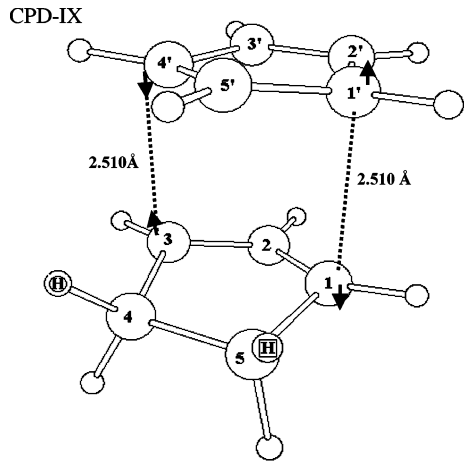

Figure 5. TS of the Cope rearrangement with *Cs* symmetry, CPD-IX.

Scheme 3. Dual Reactivity of 1,3,5-Cycloheptatriene (CHT)

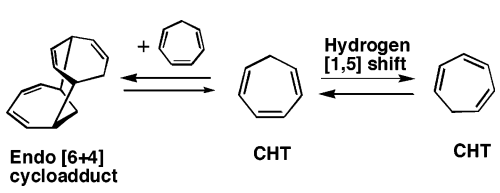

[4+2] cycloadduct was also investigated. As expected, the exo [4+2] addition TS (CPD-IVa, in Figure 3) is 1.5 kcal/mol less stable than the endo [4+2] addition TS (CPD-VI). On the other hand, the exo cycloadduct (CPD-IIIa) is 0.5 kcal/mol more stable than the endo adduct (CPD-V). From CPD-IIIa, the TS of a methylene hydrogen (denoted by a

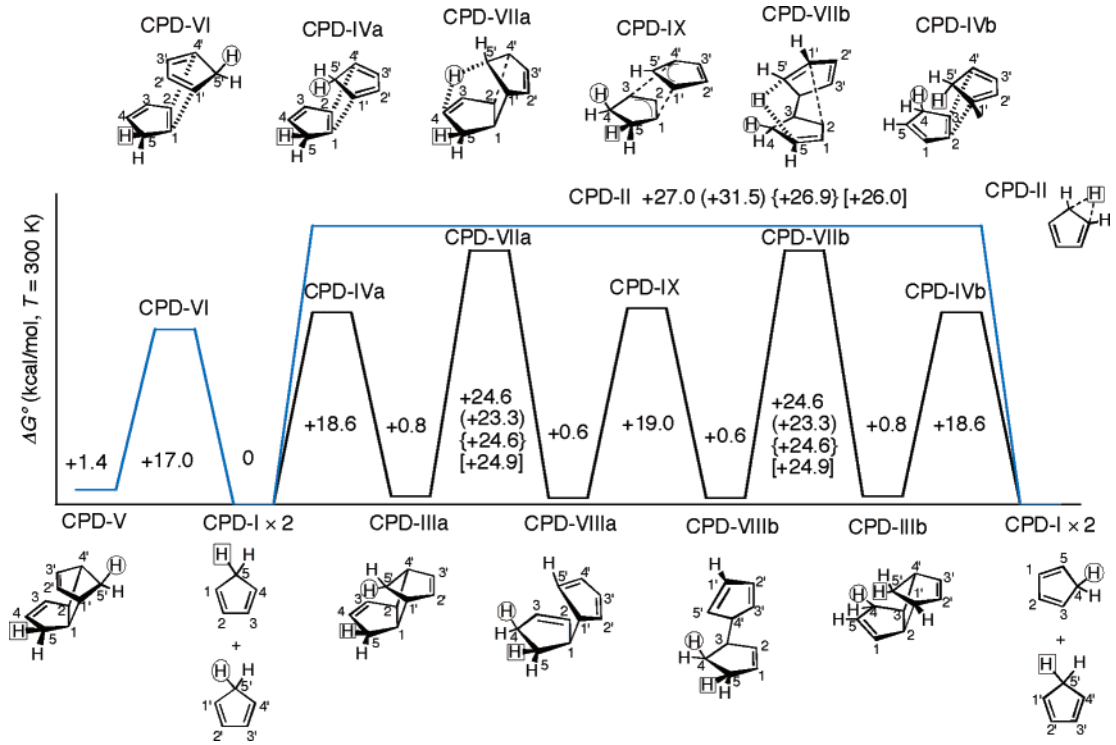

Figure 6. Changes of Gibbs free energies (RB3LYP/6-31G*, $T = 300$ K) of [4+2] cycloadditions and Cope and hydrogen [1,5] sigmatropic shifts of CPDs. Energies in parentheses were calculated by QCISD(T)/6-311G(d,p)//RB3LYP/6-31G* [QCISD(T) electronic energies and RB3LYP thermal corrections and entropies].

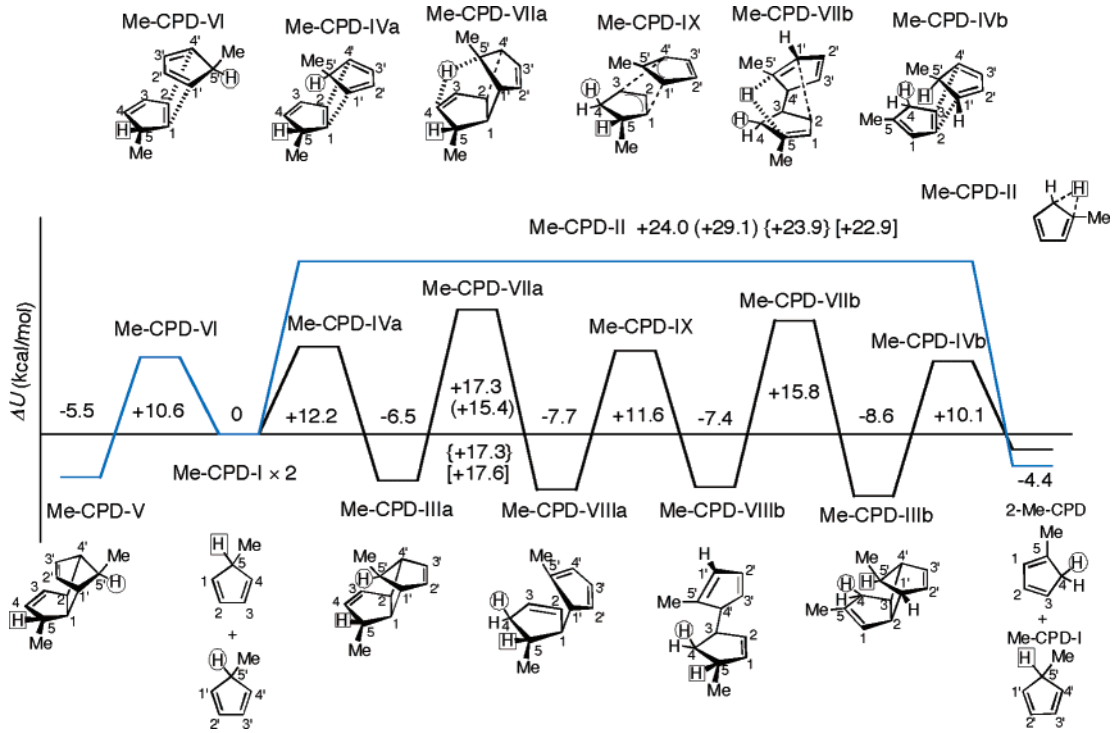

Figure 7. Changes of sums of electronic and zero-point energies (RB3LYP/6-31G*) of [4+2] cycloadditions and Cope and hydrogen [1,5] sigmatropic shifts of Me-CPD. Energies in parentheses were calculated by QCISD(T)/6-311G(d,p)//RB3LYP/6-31G* [QCISD(T) electronic energies and RB3LYP zero-point vibrational energies].

circle) migration (CPD-VIIa) was found and is shown in Figure 4. After the TS (CPD-VIIa), a one-center adduct (CPD-VIIIa) was afforded. From the adduct (CPD-VIIIa), an isomerization process (CPD-IX) was obtained and is shown in Figure 5. The process is a Cope rearrangement with *Cs* symmetry. After the Cope TS (CPD-IX), an isomer (CPD-VIIIb) that is a mirror image isomer relative to CPD-VIIIa because of the symmetry of CPD-I[17] was formed. From the one-center adduct isomer (CPD-VIIIb), a reverse route, CPD-VIIIb → CPD-VIIb → CPD-IIIb → CPD-IVb → CPD-I

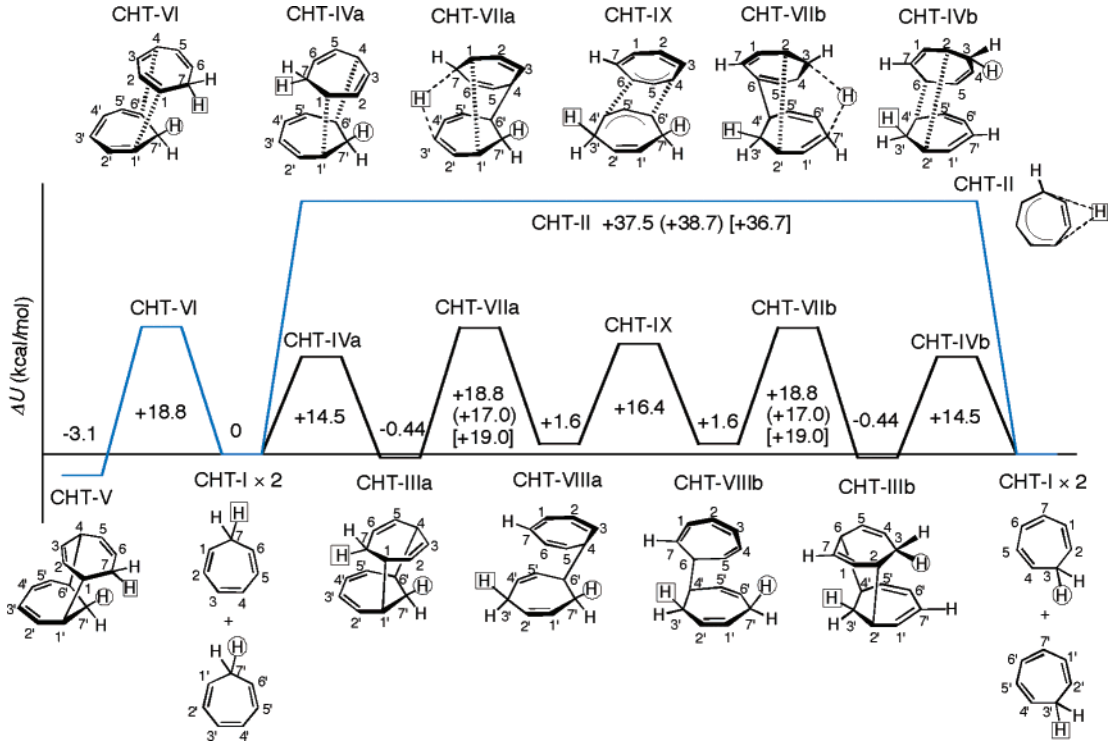

Figure 8. Changes of the sum of electronic and zero-point energies (RB3LYP/6-31G*) of [6+4] cycloadditions and Cope and hydrogen [1,5] sigmatropic shifts of CHTs. Energies in parentheses of CHT-II and CHT-VIIa,b are of QCISD(T)/6-311G(d,p)//RB3LYP/6-31G*.

+ CPD-I, is possible. As a result, a hydrogen, denoted by a circle, is [1,5] shifted (Scheme 2).

In the multistep channel, the rate-determining step is the hydrogen migration TS (CPD-VIIa or CPD-VIIb). The activation energy, $\Delta U^{\ddagger} = +17.9$ (+16.5) kcal/mol, is smaller than that of CPD-II, $\Delta U^{\ddagger} = +26.9$ (+29.4) kcal/mol. The values in parentheses are those of QCISD(T)/6-311G(d,p)//RB3LYP/6-31G*. The energy lowering due to tunnel correction[18] is 0.71 kcal/mol (CPD-II) and 0.55 kcal/mol (CPD-VIIa,b). The value ($\Delta U^{\ddagger} = +17.9$ kcal/mol) is smaller than the experimental value ($E_a = 24.3$ kcal/mol). To compare the reactivities of the unimolecular and bimolecular processes, changes of Gibbs free energies were examined and are shown in Figure 6. Although the unimolecular process is entropically more favorable than the bimolecular process, $\Delta G^{\ddagger}$ (CPD-VIIa) is smaller than $\Delta G^{\ddagger}$ (CPD-II). This result indicates that, despite the entropy loss, the present new bimolecular process is more favorable than the unimolecular process.

Next, to compare the calculation values and the experimental data further, B3LYP/6-31G* calculations of 5-methyl-1,3-cyclopentadiene (Me-CPD) were also carried out. The energy diagram is shown in Figure 7. The corresponding geometries are shown in Figures S19−S31 of the Supporting Information. Similar to CPD, the direct hydrogen shift [Me-CPD-II; $\Delta U^{\ddagger} = +24.0$ (+29.1) kcal/mol] is the most unfavorable, and the $\Delta U^{\ddagger}$ is not in agreement with the experimentally obtained activation energy ($E_a = 19.9$ kcal/mol).[19] A bimolecular route was also examined. The exo [4+2] addition TS (Me-CPD-IVa), the exo cycloadduct (Me-CPD-IIIa), the TS of a hydrogen migration (Me-CPD-VIIa), a one-center adduct (Me-CPD-VIIIa), and a Cope rearrangement TS (Me-CPD-IX) were obtained. After the Cope TS (Me-CPD-IX), a reverse route, Me-CPD-VIIIb → Me-CPD-VIIb → Me-CPD-IIIb → Me-CPD-IVb (which are not mirror image isomers because of the dissymmetry of Me-CPD-I), was obtained. Finally, 2-methyl-1,3-cyclopentadiene + Me-CPD-I were formed. The rate-determining step is the hydrogen migration TS (Me-CPD-VIIa). The activation energy, $\Delta U^{\ddagger} = +17.3$ (+15.4) kcal/mol, is in agreement with the experimentally obtained activation energy ($E_a = 19.9$ kcal/mol),[19] considering the underestimation by RB3LYP.[13] Thus, it has been shown that the hydrogen [1,5] shift of CPD takes place favorably via a bimolecular reaction.

A Bimolecular Process for the Hydrogen [1,5] Shift in CHT. 1,3,5-Cycloheptatriene (CHT) is known to undergo the hydrogen [1,5] shift at a high temperature ($T = 150$ °C).[20] In analogy with the tropone (2,4,6-cycloheptatrien-1-one)−CPD cycloaddition,[21] the dimerization of CHT is considered to be a thermally allowed [6+4] cycloaddition (Scheme 3). The 6π-electron component,[22] that is, the hexatriene moiety, is required for the reaction, because orbital lobes of FMOs (HOMO and LUMO) are largest at the triene terminal sites.

Reaction paths of cycloadditions, hydrogen [1,5] and [3,3] sigmatropic shifts, were traced. The computational energy diagram is shown in Figure 8. The TS of the direct [1,5] shift is most unstable [$\Delta U^{\ddagger} = +37.5$ (+38.7) kcal/mol; CHT-II, Figure 9]. A multistep bimolecular channel was obtained. The channel is composed of TSs of the exo [6+4] cycloaddition (CHT-IVa) in Figure 10, the hydrogen shift (CHT-VIIa) in Figure 11, a Cope shift with *Cs* symmetry (CHT-IX; Figure 12), and their mirror image isomeric reactions. Geometries of the other species, CHT-I, CHT-IIIa, CHT-VI, CHT-V, CHT-VIIIa, CHT-VIIIb, CHT-VIIb, CHT-IIIb, and CHT-IVb are shown in the Figures S10−S18 of the

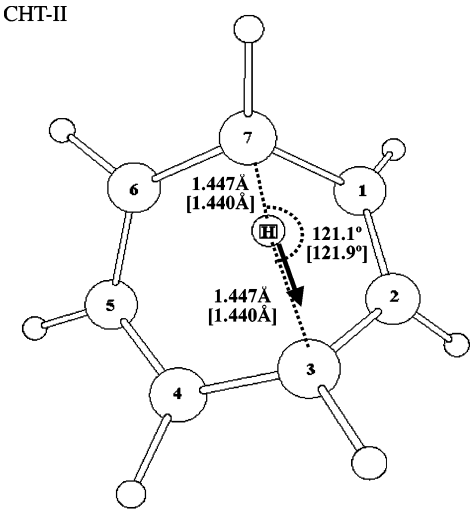

Figure 9. TS of the direct hydrogen [1,5] shift, CHT-II.

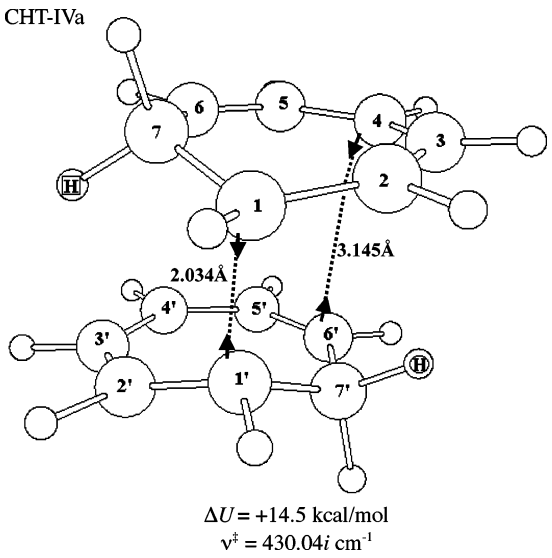

Figure 10. TS of the exo [6+4] cycloaddition, CHT-IVa. The circle and boxed hydrogens are also shown in Figure 8.

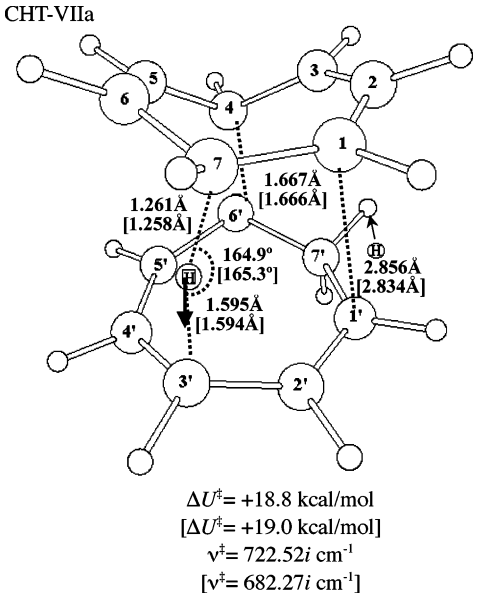

Figure 11. TS of the hydrogen shift from the exo [6+4] adduct (CHT-IIIa) to the one-center adduct intermediate (CHT-VIIIa), CHT-VIIa.

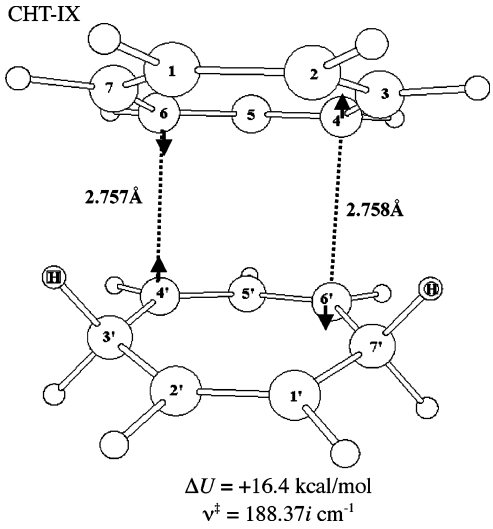

Figure 12. TS of the Cope rearrangement with *Cs* symmetry, CHT-IX.

Supporting Information. The channel leads to the double hydrogen [1,5] shifted reactants, which are located at the right edge of Figure 8 (CTH-I × 2). The rate-determining step of the channel is the hydrogen [1,5] shift [$\Delta U^{\ddagger} = +18.8$ (+17.0) kcal/mol; CHT-VIIa]. The energy lowerings by the tunnel correction are 0.98 kcal/mol (CHT-II) and 0.34 kcal/mol (CHT-VIIa,b). For a comparison containing the entropy effect, a ΔG (T = 423 K experimentally used[20]) energy diagram was depicted and is shown in Figure 13. The bimolecular process is more favorable than the unimolecular one.

B3LYP/6-31G* [QCISD/6-311G(d,p)] calculations of 7-methyl-1,3,5-cycloheptatriene (Me-CHT) were also carried out. The energy diagram of ΔU is shown in Figure 14. The corresponding geometries are shown in Figures S32−S44 in the Supporting Information. Similar to CHT, the direct hydrogen shift [Me-CHT-II; $\Delta U^{\ddagger} = +36.1$ (+37.2) kcal/mol] is the most unfavorable, and the $\Delta U^{\ddagger}$ is not in agreement with the experimentally obtained activation energy (E_a = 33.3 kcal/mol).[20b] A bimolecular route was also examined. The exo [6+4] addition TS (Me-CHT-IVa), the exo cycloadduct (Me-CHT-IIIa), the TS of a methylene hydrogen migration (Me-CHT-VIIa), a one-center adduct intermediate (Me-CHT-VIIIa), and a Cope rearrangement TS (Me-CHT-IX) were obtained. After the Cope TS (Me-CHT-IX), a reverse route, Me-CHT-VIIIb → Me-CHT-VIIb → Me-CHT-IIIb → Me-CHT-IVb, which are not mirror image isomers because of the dissymmetry of Me-CHT-I, was obtained. Finally, two 2-methyl-1,3,5-cycloheptatrienes were formed. The rate-determining step is the hydrogen migration TS (Me-CHT-VIIa). The activation energy, $\Delta U^{\ddagger} = +20.2$ (+17.3) kcal/mol, is again smaller than the experimental value (E_a = 33.3 kcal/mol). Nevertheless, the hydrogen [1,5] shift in the bimolecular route is a more favorable process in view of the comparison of the calculated energies.

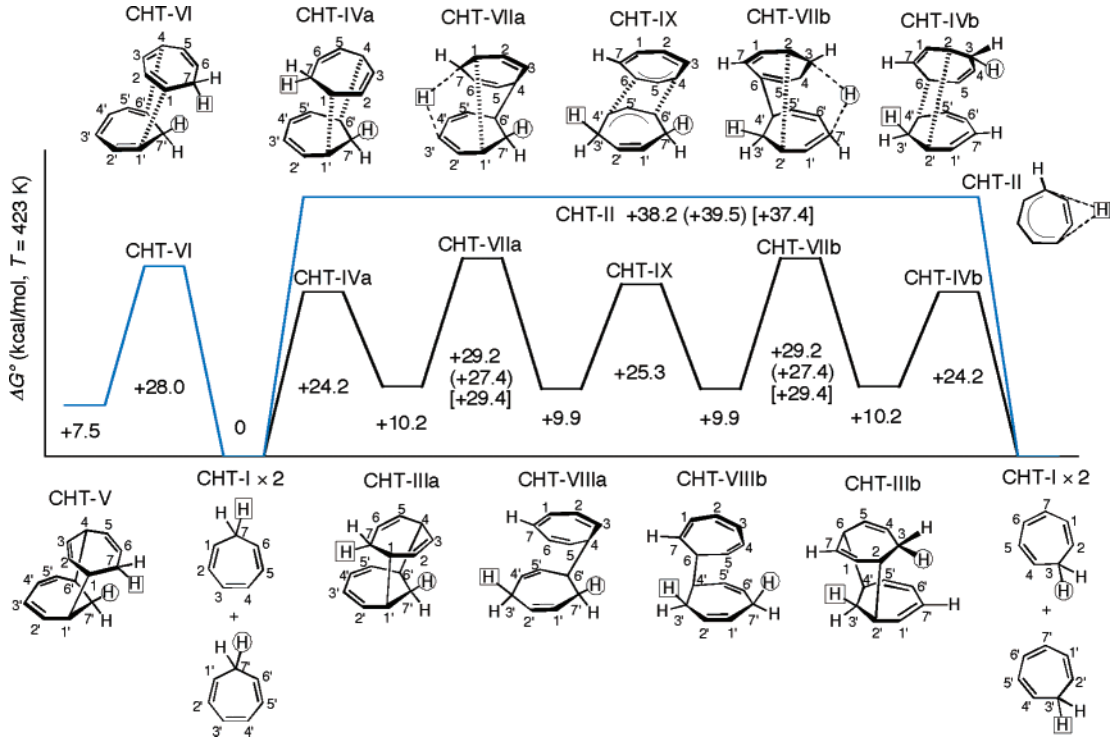

Figure 13. Changes of Gibbs free energies (RB3LYP/6-31G*, $T = 423$ K) of [6+4] cycloadditions and Cope and hydrogen [1,5] sigmatropic shifts of CHTs. Energies in parentheses were calculated by QCISD(T)/6-311G(d,p)//RB3LYP/6-31G* [QCISD(T) electronic energies and RB3LYP thermal corrections and entropies].

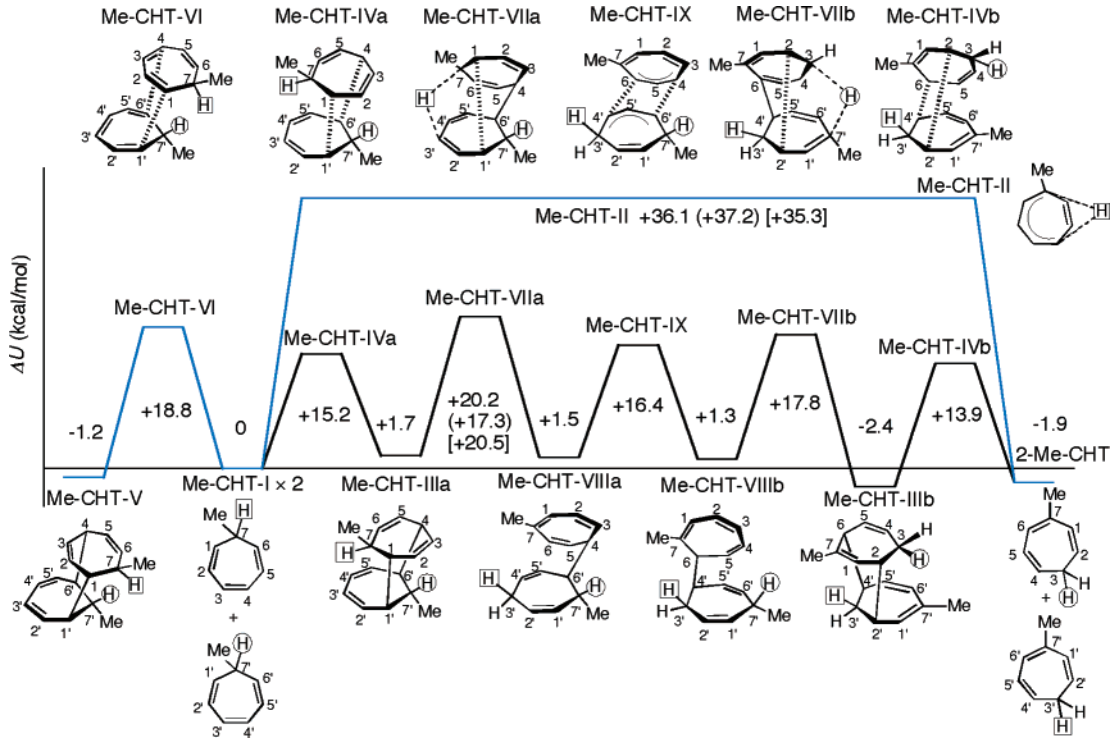

Figure 14. Changes of the sum of electronic and zero-point energies (RB3LYP/6-31G*) of [6+4] cycloadditions and Cope and hydrogen [1,5] sigmatropic shifts of Me-CHTs. Energies in parentheses of II and VIIa are of QCISD(T)/6-311G(d,p)//RB3LYP/6-31G*.

The geometries have been obtained by RB3LYP/6-31G* (gas phase) and the energies by RB3LYP/6-31G* (gas phase) and QCISD(T)/6-311G(d,p). The solvent effect has been examined for CPD and Me-CPD reactions. The data calculated by RB3LYP/6-31G* with the Onsager's reaction field are shown in braces { } in Figures 1, 2, 4, 6, and 7 and Figure S1 (Supporting Information). Since the dielectric constant of CCl_4 is small (= 2.228), the reaction field containing geometries are almost the same as those in the gas phase. Also, the energy changes are insensitive to the

Scheme 4. CT and Back CT Interactions Leading to the Hydrogen Shift. In A, Those of CPD-II Are Depicted. In B, Those of the [1,5] H Shift in 1,3-Pentadiene Are Shown. In C, Those of CPD-VIIa Are Exhibited. Through CT, the C−H Bonding Becomes Weakened and the New C−H Bond Is Formed. Also, through Back CT, the Same Bond Interchange Is Induced.

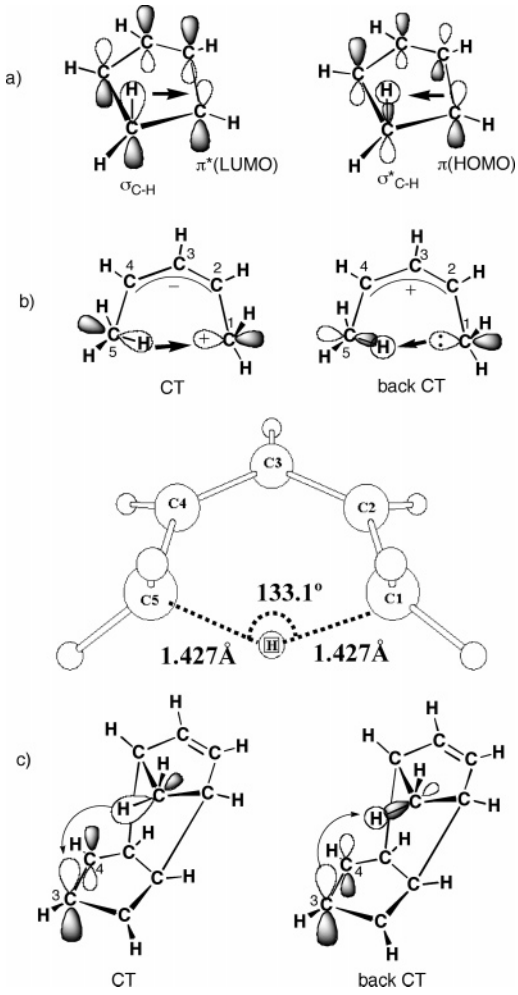

presence or absence of the effect. For instance, $\Delta U^{\ddagger} = +26.9$ kcal/mol (gas phase) is nearly equal to $\{\Delta U^{\ddagger} = +26.8$ kcal/mol (reaction field)$\}$ for CPD-II in Figure 1.

The effect of the polarization's function on the migrating hydrogen atom on the geometries and energies has been examined. The data are shown in square brackets [ ]. For the TS geometries, the effect has been found to be negligible. For instance, in Figure 4, C(4)···H distances are 1.589 Å and [1.590 Å] and C(5′)−H distances are 1.260 Å and [1.257 Å]. The energies vary by, at most, 1 kcal/mol. For example, $\Delta U^{\ddagger} = +26.9$ kcal/mol and $[\Delta U^{\ddagger} = +25.8$ kcal/mol] for CPD-II and $\Delta U^{\ddagger} = +17.9$ kcal/mol and $[\Delta U^{\ddagger} = +18.1$ kcal/mol] for CPD-VIIa in Figure 1. Thus, Onsager's reaction field and the polarization function on the migrating hydrogen atom have only a small effect on the calculated geometries and energies.

FMO Interactions for the Hydrogen Shift. In this subsection, the bimolecular process is considered in terms of the frontier-orbital interactions. Scheme 4 presents three types of the FMO interactions. In Scheme 4a, the hydrogen [1,5] shift is described by charge transfer (CT) from the sp^3 C−H bonding orbital to the diene LUMO and by back CT from the diene HOMO to the C−H antibonding vacant orbital. To cause the effective CT and back CT, large orbital overlaps are required. But, the CT in Scheme 4a suffers a small overlap owing to the nearly parallel expansion. To make the matter worse, in back CT, the overlap is almost canceled out as a result of the node of σ^*_{C-H}. Thus, the ring-strained FMO interactions are unfavorable. In Scheme 4b, CT and back CT in 1,3-pentadiene are shown. The p_π atomic orbital of the right-sided terminal methylene group may be directed to the left-sided C−H bond of the methyl group. The direction leads to the large orbital overlaps for CT and back CT, and consequently, the unimolecular [1,5] H shift is likely. In Scheme 4c, those interactions in the stacked [4+2] exo dimer of CPD, CPD-VIIa, are shown. The C−H bonding and antibonding orbitals are directed suitably to π and π^* orbitals of the C_3═C_4 bond. The σ-type orbital overlaps become feasible in the stacked form of the exo [4+2] cycloadduct. The C···H···C angle in CPD-VIIa (149.1°, Figure 4) is larger than that in 1,3-pentadiene (133.1°, Scheme 4b), and the CPD dimer provides a ground for the facile H shift. Interestingly, the sum of two C···H distances, 1.260 + 1.589 Å, in CPD-VIIa is very close to that, 1.427 + 1.427 Å, in 1,3-pentadiene (Scheme 4b).

Conclusion

Novel multistep channels for the hydrogen [1,5] shifts for CPD and CHT have been shown. The present results suggest new aspects for pericyclic reactions. The suggestion is that ring-strained methylene hydrogen may shift favorably in the [4+2] or [6+4] stacked conformation. Cycloadditions, sigmatropic shifts, and their reverse reactions work cooperatively to give hydrogen [1,5] shifts for the cycloaddition-favored reactants.

Supporting Information Available: The energy diagrams and optimized geometries not shown in Figures 1−14 for CPD, CHT, Me-CPD, and Me-CHT. This material is available free of charge via the Internet at http://pubs.acs.org.

References

(1) Woodward, R. B.; Hoffmann, R. *The Conservation of Orbital Symmetry*; Verlag Chemie: New York, 1970.

(2) (a) Fukui, K. *Theory of Orientation and Stereoselection*; Springer: New York, 1970. (b) Fleming, I. *Frontier Orbitals and Organic Chemical Reactions*; John Wiley & Sons: New York, 1976.

(3) Houk, K. N.; Li, Y.; Evanseck, J. D. *Angew. Chem., Int. Ed. Engl.* **1992**, *31*, 682.

(4) Spangler, C. W. *Chem. Rev.* **1976**, *76*, 187.

(5) (a) Dormans, G. J. M.; Buck, H. M. *J. Mol. Struct.* **1986**, *136*, 121. (b) Dormans, G. J. M.; Buck, H. M. *J. Am. Chem. Soc.* **1986**, *108*, 3253. (c) Hess, B. A., Jr.; Schaad, L. J.; Pancir, J. *J. Am. Chem. Soc.* **1985**, *107*, 149. (d) Hess, B. A., Jr.; Schaad, L. J. *J. Am. Chem. Soc.* **1983**, *105*, 7185. (e) Dewar, M. J. S.; Merz, J. M.; Stewart, J. J. P. *J. Chem. Soc., Chem. Commun.* **1985**, 166. (f) Castenmiller, W. A. M.; Buck, H. M. *Tetrahedron* **1979**, *35*, 397. (g) Jensen, F. J.; Houk, K. N. *J. Am. Chem. Soc.* **1987**, *109*, 3139. (h) Dewar, M. J. S.; Healr, E. F.; Merz, J. M. *J. Am. Chem. Soc.* **1988**, *110*, 2666.

(6) Diels, O.; Alder, K. *Justus Liebigs Ann. Chem*. **1928**, *460*, 98.

(7) (a) Wassermann, A. *Diels−Alder Reactions*; Elsevier: London, 1965. (b) Sangwan, N. K.; Schneider, H.-J. *J. Chem. Soc., Perkin Trans. 2*. **1989**, 1223. (c) Jorgensen, W. L.; Blake, J. F.; Lim, D.; Severance, D. L. *J. Chem. Soc., Faraday Trans.* **1994**, *90*, 1727. (d) Breslow, R.; Zhu, Z. *J. Am. Chem. Soc*. **1995**, *117*, 9923.

(8) Alder, K.; Ache, H. J. *Chem. Ber*. **1962**, *95*, 503; 511.

(9) (a) Kahn, S. D.; Hehre, W. J.; Rondan, N. G.; Houk, K. N. *J. Am. Chem. Soc*. **1985**, *107*, 8291. (b) Rondan, N. G.; Houk, K. N. *Tetrahedron Lett*. **1984**, *25*, 2519. (c) Bachrach, S. M. *J. Org. Chem*. **1993**, *58*, 5414. (d) Okajima, T.; Imafuku, K. *J. Org. Chem*. **2002**, *67*, 625.

(10) (a) Caramella, P.; Quadrelli, P.; Toma, L. *J. Am. Chem. Soc*. **2002**, *124*, 1130. (b) Jamróz, M.; Galka, S.; Dobrowolski, J. C. *THEOCHEM* **2003**, *634*, 225.

(11) Roth, W. R. *Tetrahedron Lett*. **1964**, 1009.

(12) Roth, W. R.; Konig, J. *Justus Liebigs Ann. Chem*. **1966**, *699*, 24.

(13) Lynch, B. J.; Fast, P. L.; Harris, M.; Truhlar, D. G. *J. Phys. Chem. A* **2000**, *104*, 4811.

(14) Becke, A. D. *J. Chem. Phys*. **1993**, *98*, 5648.

(15) Frisch, M. J.; Trucks, G. W.; Schlegel, H. B.; Scuseria, G. E.; Robb, M. A.; Cheeseman, J. R.; Zakrzewski, V. G.; Montgomery, J. A., Jr.; Stratmann, R. E.; Burant, J. C.; Dapprich, S.; Millam, J. M.; Daniels, A. D.; Kudin, K. N.; Strain, M. C.; Farkas, O.; Tomasi, J.; Barone, V.; Cossi, M.; Cammi, R.; Mennucci, B.; Pomelli, C.; Adamo, C.; Clifford, S.; Ochterski, J.; Petersson, G. A.; Ayala, P. Y.; Cui, Q.; Morokuma, K.; Salvador, P.; Dannenberg, J. J.; Malick, D. K.; Rabuck, A. D.; Raghavachari, K.; Foresman, J. B.; Cioslowski, J.; Ortiz, J. V.; Baboul, A. G.; Stefanov, B. B.; Liu, G.; Liashenko, A.; Piskorz, P.; Komaromi, I.; Gomperts, R.; Martin, R. L.; Fox, D. J.; Keith, T.; Al-Laham, M. A.; Peng, C. Y.; Nanayakkara, A.; Challacombe, M.; Gill, P. M. W.; Johnson, B.; Chen, W.; Wong, M. W.; Andres, J. L.; Gonzalez, C.; Head-Gordon, M.; Replogle, E. S.; Pople, J. A. *Gaussian 98*, Revision A.11.1; Gaussian, Inc.: Pittsburgh, PA, 2001.

(16) Onsager, L. *J. Am. Chem. Soc*. **1938**, *58*, 1486.

(17) The geometries of CPD-IVb, CPD-IIIb, CPD-VIIb, and CPD-VIIIb were made by changing all the signs of the Cartesian coordinates of the geometries of CPD-IVa, CPD-IIIa, CPD-VIIa, and CPD-VIIIa. The energies of CPD-IVb, CPD-IIIb, CPD-VIIb, and CPD-VIIIb are the same as those of CPD-IVa, CPD-IIIa, CPD-VIIa, and CPD-VIIIa.

(18) Wigner, E. P. *Phys. Chem*. **1933**, *B19*, 203.

(19) McLean, S.; Webster, C. J.; Rutherford, R. J. D. *Can. J. Chem*. **1969**, *47*, 1555.

(20) (a) Ter Borg, A. P.; Razenberg, E.; Kloosterziel, H. *Recl. Trav. Chim. Pays-Bas* **1965**, *84*, 1230. (b) Egger, K. W. *J. Am. Chem. Soc*. **1967**, *89*, 3688.

(21) (a) Cookson, R. C.; Drake, B. V.; Hudec, J.; Morrison, A. *J. Chem. Soc., Chem. Commun*. **1966**, 15. (b) Ito, S.; Fujise, Y.; Okuda, T.; Inoue, Y. *Bull. Chem. Soc. Jpn*. **1966**, *39*, 1351.

(22) CHT has a geometric isomer, bicyclo[4.1.0]hepta-2,4-diene (norcaradiene, NCD). NCD has a puckered conformation, which is apparently suitable for the intramolecular hydrogen shift. However, NCD cannot be a reactant for the hydrogen shift, because the cyclopropyl ring in NCD precludes the hydrogen-bridged TS structure. Cycloadditions between CHT and NCD were calculated and are less stable than the rate-determining step VIIa,b in Figure 8. A series of isomerizations of methyl-NCDs were observed. They would involve intermediates of cycloadducts of two methyl-CHTs. (a) Berson, J. A.; Willcot, M. R., III; *J. Am. Chem. Soc*. **1965**, *87*, 2751. (b) Berson, J. A.; Willcot, M. R., III; *J. Am. Chem. Soc*. **1965**, *87*, 2752.

CT0500646